Desalination and Water Treatment
www.deswater.com

doi: 10.1080/19443994.2015.1091997

57 (2016) 18694–18709
August

Taylor & Francis
Taylor & Francis Group

A detailed study on adsorption isotherms of Hg(II) removal from aqueous solutions using nanostructured sorbent $ZnCl_2$-MCM-41

Foad Raji[a,*], Majid Pakizeh[a], Alireza Saraeian[b], Mojtaba Raji[c]

[a]*Faculty of Engineering, Department of Chemical Engineering, Ferdowsi University of Mashhad, P.O. Box 91775-1111, Mashhad, Iran, Tel./Fax: +98 2176510633; emails: Foad.raji@gmail.com (F. Raji), Pakizeh@um.ac.ir (M. Pakizeh)*
[b]*Chemical & Materials Engineering Department, New Mexico State University, Las Cruces, NM 88003, USA, email: alirezas@nmsu.edu*
[c]*Separation Processes Research Group (SPRG), Department of Engineering, University of Kashan, P.O. Box 873175-1167, Kashan, Iran, email: Mojtabaraji90@gmail.com*

Received 23 March 2015; Accepted 2 September 2015

ABSTRACT

A comparison between linear and non-linear regression methods to determine the optimum isotherm was done by applying these models to the experimental equilibrium data of Hg(II) sorption using new nanostructured sorbent $ZnCl_2$–MCM-41. The best-fitting linear isotherm was selected based on the highest R^2 value obtained. In the case of non-linear methods, different error functions were employed to determine the best-fitting model. Langmuir isotherm was found to be the best-fitting model in both linear and non-linear cases, which implies a monolayer adsorption of Hg(II) onto a homogeneous surface of $ZnCl_2$–MCM-41. Scanning electron microscopic images verified the spherical morphology of the sorbent particles. The adsorption capacities of Hg(II) onto $CaCl_2$–MCM-41, $CuCl_2$–MCM-41, and $MgCl_2$–MCM-41 were demonstrated to be less than those of $ZnCl_2$–MCM-41. Lastly, Hg(II) recovery of up to 75% was obtained by utilizing 0.1 M HNO_3 solution.

Keywords: Nanostructured sorbent; $ZnCl_2$-MCM-41; Hg(II) removal; Non-linear regression; Isotherm; Adsorption capacity

1. Introduction

Water pollution by toxic heavy metals has become a critical environmental issue over the past few decades. One of the most toxic heavy metals is mercury, which exists in three chemical forms, namely elemental mercury, inorganic mercurous and mercuric forms (Hg(I) and Hg(II)), and organic alkyl mercury. In particular, mercury remarkably affects neurological and renal activities, which necessitates the removal of mercury from wastewater before its discharge into the environment. Adsorption, as a wastewater treatment process, has been found to be an economically feasible approach for Hg(II) ion removal [1]. Different sorbents, such as silica gel [2], chelating resins [3], metal oxides [4], activated carbon [5], and MCM-41 [6] have been used to sequester Hg(II) from aqueous solutions. MCM-41, the most widely used member of mesostructured silica, was first introduced in 1992, as a result of the self-assembly of a structure directing agent and the silica source [7]. A regular array of uniform pores, controllable pore size, and the ability to functionalize

---

*Corresponding author.

the surface for particular separations are the main features of MCM-41.

In this work, MCM-41 particles are synthesized through the hydrothermal method, and then $ZnCl_2$ particles are incorporated into its pores. This new hybrid sorbent, known as $ZnCl_2$–MCM-41 is then applied for Hg(II) removal from aqueous solution. More information about the synthesis and characterization of the nanostructure sorbent and also the effect of operation parameters on mercury removal by $ZnCl_2$–MCM-41 is discussed in detail in our previous work [8]. The purpose of this study is to discuss the adsorption isotherms, especially the adsorption capacity of sorbents, in depth. The linear least-squared method and non-linear isotherm models are compared (isotherms are listed in Table 1). In addition, Hg(II) adsorption capacity of $ZnCl_2$–MCM-41 sorbent is evaluated and compared to some of the sorbents reported previously. Furthermore, the effects of ionic strength, sorbent dosage, and the incorporation of other metal salts onto MCM-41 are investigated. Finally, desorption studies are performed to assess the recovery of Hg(II).

2. Materials and methods

2.1. Synthesis of the adsorbent material

The complete synthesis processes of MCM-41 and $ZnCl_2$–MCM-41 are presented in our previous study [8].

2.2. Preparation of metal solutions

A stock solution of Hg(II) was prepared by dissolving 1.354 g of $HgCl_2$ in 1 l of deionized water. Other concentrations were prepared from stock solution by dilution, varying between 2 and 50 mg L^{-1}, and the pH of the working solutions was adjusted to desired values with 0.1 M nitric acid or 0.1 M sodium hydroxide. Fresh dilutions were used for each experiment. All chemicals used were of analytical grade.

2.3. Adsorption experiments using batch study

Batch adsorption experiments were conducted by placing 10 mg of hybrid $ZnCl_2$–MCM-41 sorbent in a series of Erlenmeyer flasks each containing 30 ml of the metal containing solution at specific initial concentrations and pH values. The contents of the flasks were then magnetically stirred for a specific time at the rate of 300 rpm with controlled temperature during the adsorption process. After filtering the samples through Whatman No. 42 filter papers, the residual concentration of Hg(II) in the solution was determined by atomic absorption spectroscopy (atomic absorption/flame emission spectrophotometer Shimadzu AA-670). The amount of Hg(II) adsorption per gram of the $ZnCl_2$–MCM-41 was calculated according to Eq. (1):

$$q_e = \frac{(C_0 - C_e)V}{m} \tag{1}$$

where q_e is the adsorption capacity (mg g^{-1}), V is the volume of the solution (L), m is the mass of the dry sorbent (g), and C_0 and C_e are the initial and equilibrium metal concentrations, respectively (mg L^{-1}).

2.4. Adsorption isotherms

Isotherms are relationships between equilibrium adsorption amounts and equilibrium concentrations, which are obtained by examining batch reactions at constant temperature. The adsorption capacity of a

Table 1
Isotherm models and their linear forms

Isotherm	Nonlinear form	Linear form	Plot
Langmuir	$q_e = \frac{q_m K_L C_e}{1+K_L C_e}$	$\frac{C_e}{q_e} = \frac{1}{K_L q_m} + \frac{1}{q_m} C_e$	$\frac{C_e}{q_e}$ vs. C_e
Freundlich	$q_e = K_F C_e^{1/n}$	$\ln q_e = \ln K_F + \frac{1}{n} \ln C_e$	$\ln q_e$ vs. $\ln C_e$
Temkin	$q_e = \frac{RT}{b} \ln(K_T C_e)$	$q_e = \frac{RT}{b} \ln K_T + \frac{RT}{b} \ln C_e$	q_e vs. $\ln C_e$
Sips	$q_e = \frac{q_m K_S C_e^{1/n}}{1+K_S C_e^{1/n}}$	$\ln\left(\frac{q_m}{q_e} - 1\right) = -\ln K_S - \frac{1}{n} \ln C_e$	$\ln\left(\frac{q_m}{q_e} - 1\right)$ vs. $\ln C_e$
R–P	$q_e = \frac{K_{RP} C_e}{1+a_{RP} C_e^{\beta}}$	$\ln\left(\frac{K_{RP} C_e}{q_e} - 1\right) = \ln a_{RP} + \beta \ln C_e$	$\ln\left(\frac{K_{RP} C_e}{q_e} - 1\right)$ vs. $\ln C_e$
Toth	$q_e = \frac{q_m C_e}{(K_{T0}+C_e^{\mu})^{1/\mu}}$	$\ln\left(\frac{q_e}{q_m}\right) = \ln C_e - \frac{1}{\mu} \ln\left(K_{T0} + C_e^{\mu}\right)$	–
Khan	$q_e = \frac{q_m b_K C_e}{(1+b_K C_e)^{\gamma}}$	$\ln\left(\frac{q_e}{q_m}\right) = \ln C_e + \ln \frac{b_K}{(1+b_K C_e)^{\gamma}}$	–

sorbent is determined by isotherm equation and is a good criterion to compare the metal removal efficiency of different sorbents. The Langmuir and Freundlich are the most common isotherm models used to describe adsorption equilibrium data. In fact, no theoretical adsorption isotherm exists to describe adsorption in liquid phase. Hence, gas adsorption isotherm models are used to describe liquid-phase adsorption data [9]. Additionally, different sorption isotherm models—namely Temkin, Sips, Redlich–Peterson (R–P), Toth, and Khan—have been applied to the experimental data obtained from batch equilibrium tests. Linear regression methods are frequently used to determine the best-fitting isotherm equation. Linear least squares method is the most commonly used method for linearly transformed isotherm equations to confirm the experimental data by employing coefficients of determinations. The coefficient of determination (R^2) for linear regression models is the most commonly used parameter to investigate the correlation between the experimental data and the predicted isotherm value. However, transformation of non-linear isotherm equations to linear forms alters their error structure and may also vary the error variance, and violate the assumption of normality in standard least squares [10]; therefore, the non-linear regression method is found to be the best in selecting the optimum isotherm [11,12]. In this method, in order to find a set of isotherm kinetic parameters, the error distribution between the experimental data and the predicted isotherm is minimized (maximized in case of coefficient of determination). Consequently, a trial-and-error procedure is developed to determine the kinetic parameters using an optimization routine in the *solver add-in* of Microsoft's spreadsheet, Excel. Seven error functions were employed in this study to evaluate the goodness-of-fit of the equations to the experimental data. These error functions are: the coefficient of determination (R^2), nonlinear chi-square test (χ^2), residual root mean square error (RMSE), average relative error (ARE), standard deviation of relative error (S_{RE}), Marquardt's percent standard deviation (MPSD), and the sum of the squares of the errors (ERRSQ) [13]. After computing these error functions for each isotherm, the sum of normalized errors (SNE) is calculated for each case, and finally the smallest SNE indicates the optimal isotherm. The calculation for the "sum of the normalized errors" is as follows:

(1) Select one isotherm and one error function (for example, ERRSQ error function) and get the *solver add-in* output to determine the isotherm parameters in a way that minimizes the applied error function (in this case, ERRSQ). (If the applied error function is the coefficient of determination, the *solver add-in* must be adjusted on maximizing).
(2) The values of other error functions are determined based on isotherm parameters obtained from step (1).
(3) The above steps are performed exactly for all other error functions.
(4) The maximum output of each error function is selected from among all sets. In order to calculate the normalized error, the value of other sets should be divided by the maximum value. This should be done for all error functions.
(5) The summation of all of these normalized errors for each parameter set is calculated.

The error function equations are presented in Table 2.

2.5. Desorption studies

0.1 g of $ZnCl_2$–MCM-41 sorbent samples that was used for the removal of 2, 5, 10, 20, and 50 mg L^{-1} of 30 ml Hg(II) solutions were filtered using Whatman No. 42 filter papers. Subsequently, the Hg(II)-loaded $ZnCl_2$–MCM-41 samples were transferred into conical flasks containing 200 ml of the 0.1 M HNO_3 solution. The flasks were covered immediately, and then sonicated for 60 min at 60°C. The amount of Hg(II) remaining in the solutions was determined by atomic absorption spectrophotometer.

3. Results and discussion

It is necessary to state that the effect of operating conditions, such as pH, temperature, contact time, initial metal concentration, and foreign ions on Hg(II) sorption and also, the kinetic parameters were studied comprehensively in our previous papers [8,15].

The isotherm models were fitted to the experimental data in order to obtain more information about the process, including maximum theoretical uptake capacity, dominant mechanisms of the adsorption process, data on physisorption and chemisorption, and determination of monolayer or multilayer adsorption.

3.1. Linear regression method

The linear regression of experimental data is the simplest way to determine isotherm constants for two-parameter isotherms. The Langmuir, Freundlich, and Temkin models are two-parameter adsorption models, which could easily be transformed to linear forms, and their constants can be calculated without any trial

Table 2
List of error functions [14]

Error function	Abbreviation	Definition/expression
The coefficient of determination	R^2	$R^2 = \frac{\sum\left(q_{\mathrm{e,meas}} - \bar{q}_{\mathrm{e,calc}}\right)^2}{\sum\left(q_{\mathrm{e,meas}} - \bar{q}_{\mathrm{e,calc}}\right)^2 + \sum\left(q_{\mathrm{e,meas}} - q_{\mathrm{e,calc}}\right)^2}$
Nonlinear chi-square test	χ^2	$\chi^2 = \sum_{\mathrm{i}=1}^{n} \frac{\left(q_{\mathrm{e,meas}} - q_{\mathrm{e,calc}}\right)^2}{q_{\mathrm{e,meas}}}$
Residual root mean square error	RMSE	$\mathrm{RMSE} = \sqrt{\frac{1}{n-2}\sum_{\mathrm{i}=1}^{n}\left(q_{\mathrm{e,meas}} - q_{\mathrm{e,calc}}\right)^2}$
Average relative error	ARE	$\mathrm{ARE} = \frac{100}{n}\sum_{\mathrm{i}=1}^{n}\left\lvert\frac{q_{\mathrm{e,meas}} - q_{\mathrm{e,calc}}}{q_{\mathrm{e,meas}}}\right\rvert$
Standard deviation of relative errors	S_{RE}	$S_{\mathrm{RE}} = \sqrt{\frac{\sum_{\mathrm{i}=1}^{n}\left[\left(q_{\mathrm{e,meas}} - q_{\mathrm{e,calc}}\right) - \mathrm{ARE}\right]^2}{n-1}}$
Marquardt's percent standard deviation	MPSD	$\mathrm{MPSD} = 100\sqrt{\frac{1}{n-p}\sum_{\mathrm{i}=1}^{n}\left(\frac{q_{\mathrm{e,meas}} - q_{\mathrm{e,calc}}}{q_{\mathrm{e,meas}}}\right)^2}$
Sum squares errors	ERRSQ	$\mathrm{ERRSQ} = \sum_{\mathrm{i}=1}^{n}\left(q_{\mathrm{e,meas}} - q_{\mathrm{e,calc}}\right)^2$

and error. The Sips and R–P isotherm models are three-parameter models, both of which require a trial-and-error step for linearization. Toth's and Khan's isotherm equations include three adjustable parameters and cannot be fitted to the experimental data by linear regression. Among these models, the Langmuir isotherm has more than one linear form: four common and different linearized forms of the Langmuir model are listed in Table 3. The Langmuir-1 isotherm model is more common than other forms. The four different linearized forms of the Langmuir isotherm were analyzed to investigate the effect of transformation from non-linear to linear form. Isotherm model parameters and the coefficients of determination for various adsorption isotherms are presented in Table 4. Higher values for the coefficient of determination indicate a stronger correlation between the experimental data and the isotherm model. In the case of the R–P and Sips isotherms, the constants K_{RP} and q_{m} were obtained by maximizing the R^2 value using a trial-and-error step in the *solver add-in* function of Microsoft Excel, Microsoft Corporation. Fig. 1 shows the plot of isotherms predicted by the linear regression method.

As can be seen in Table 4, all linearized Langmuir equations have high R^2 values (higher than 0.997), while the Langmuir-1 isotherm model has the highest R^2 value. Moreover, the R^2 values attained for all Langmuir models were higher than those of the Freundlich, Temkin, and R–P isotherms, indicating that

Table 3
Various linear forms of the Langmuir isotherm equation

Isotherm	Linear form	Plot
Langmuir-1	$\frac{C_{\mathrm{e}}}{q_{\mathrm{e}}} = \frac{1}{K_{\mathrm{L}}q_{\mathrm{m}}} + \frac{1}{q_{\mathrm{m}}}C_{\mathrm{e}}$	$\frac{C_{\mathrm{e}}}{q_{\mathrm{e}}}$ vs. C_{e}
Langmuir-2	$\frac{1}{q_{\mathrm{e}}} = \frac{1}{K_{\mathrm{L}}q_{\mathrm{m}}}\frac{1}{C_{\mathrm{e}}} + \frac{1}{q_{\mathrm{m}}}$	$\frac{1}{q_{\mathrm{e}}}$ vs. $\frac{1}{\mathrm{Ce}}$
Langmuir-3	$q_{\mathrm{e}} = -\frac{1}{K_{\mathrm{L}}}\frac{q_{\mathrm{e}}}{C_{\mathrm{e}}} + q_{\mathrm{m}}$	q_{e} vs. $\frac{q_{\mathrm{e}}}{C_{\mathrm{e}}}$
Langmuir-4	$\frac{q_{\mathrm{e}}}{C_{\mathrm{e}}} = -K_{\mathrm{L}}q_{\mathrm{e}} + K_{\mathrm{L}}q_{\mathrm{m}}$	$\frac{q_{\mathrm{e}}}{C_{\mathrm{e}}}$ vs. q_{e}

Table 4
Isotherm parameters for various two parameters adsorption isotherms for the adsorption of Hg(II) onto $ZnCl_2$–MCM-41 at 25°C and pH 10

Isotherm models	Parameters	Value
Langmuir-1	q_m (mg g^{-1})	204.1
	K_L (L mg^{-1})	0.084
	R^2	0.9995
Langmuir-2	q_m (mg g^{-1})	178.7
	K_L (L mg^{-1})	0.097
	R^2	0.9986
Langmuir-3	q_m (mg g^{-1})	200.7
	K_L (L mg^{-1})	0.086
	R^2	0.9976
Langmuir-4	q_m (mg g^{-1})	201.1
	K_L(L mg^{-1})	0.085
	R^2	0.9976
Freundlich	K_F	14.975
	$1/n$	0.8062
	R^2	0.9810
Temkin	b (J mol^{-1})	89.92
	K_T	2.39
	R^2	0.9009
Sips	q_m (mg g^{-1})	203.2
	K_S	0.0845
	n	1.00
	R^2	0.9999
R–P	K_{RP}	17.7
	a_{RP}	0.1215
	β	0.8721
	R^2	0.9975

the Langmuir equation offers better prediction of Hg(II) sorption by $ZnCl_2$–MCM-41 than the other three models. Nevertheless, the R^2 value for the Sips isotherm was higher than that of the Langmuir model, suggesting that the linear form of the Sips isotherm fits better to the experimental data. Consequently, the nature of the adsorption of Hg(II) ions onto $ZnCl_2$–MCM-41 is more compatible with the assumptions of the Sips isotherm.

It should be noted that when the parameter n in the Sips model is equal to 1.0, this model is essentially equivalent to the Langmuir isotherm. In fact, the Sips model was the first effort to extend the Langmuir model to adsorption on an energetically heterogeneous solid based on the assumption of quasi-Gaussian energy distribution, where the ε ($\varepsilon = 1/n$) factor shows the surface heterogeneity ($\varepsilon = 1$ means a completely homogeneous surface and $\varepsilon < 1$ shows the heterogeneity of the surface) [16]. At small amounts of ε (close to zero), the Sips model is the same as the Freundlich isotherm. Consequently, high R^2 values of the Sips and Langmuir models (which have similar fundamentals at $\varepsilon = 1$) indicate monolayer adsorption of Hg(II) species onto the homogeneous surface of the $ZnCl_2$–MCM-41 sorbent.

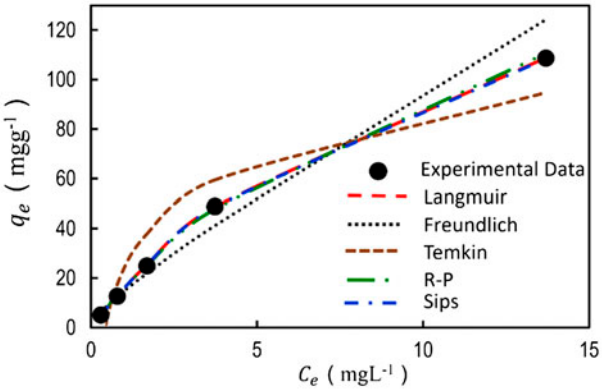

Fig. 1. Experimental data and the predicted Langmuir, Freundlich, Temkin, R-P, and Sips isotherms by linear regression method.

An important point in Table 4 is the difference among the values obtained for the four linear forms of the Langmuir isotherm, especially the major difference between Langmuir-2 and the other three forms. This point provides evidence that different linearization methods can change the error distribution structure of a model. The difference in the obtained values for R^2 and q_e proves the change in the error structure of models after linearization, which makes the selection of the best-fitted isotherm difficult. Consequently, it is suggested that the highest coefficient of determination (R^2) does not necessarily imply the best fit, but instead shows the model whose error distribution is closest to the "true error distribution" [17].

3.2. Non-linear regression method

All the non-linear model parameters were evaluated by non-linear regression analysis using the *solver add-in* from Microsoft's spreadsheet, Excel. Linearization of non-linear experimental data sometimes changes the error distribution structure of the isotherms. As a result, some researchers have proposed the non-linear method as a better way to obtain the isotherm parameters [11,12,18–21]. The comparison of isotherms by non-linear regression is more reliable than the linear regression method because the experimental equilibrium data and the isotherms are in a fixed x and y axis and no transformation error takes place during regression. Here, each one of the R^2, χ^2, RMSE, S_{RE}, MPSD, and ERRSQ error functions were selected as an optimal function, and other error functions were computed based on the selected error function.

3.2.1. The Langmuir isotherm

The Langmuir isotherm constants and error values determined by non-linear regression based on different error functions are presented in Table 5. The q_{m} and K_{L} values calculated based on different error functions are very close to each other, indicating that the Langmuir isotherm accurately predicts the equilibrium behavior of Hg(II) sorption by $ZnCl_2$-MCM-41. Moreover, the predicted values for q_{m} and K_{L} are approximately similar in type 1, type 3, and type 4 of the linear forms of the Langmuir isotherm. The R^2 value obtained in the non-linear method was higher than that of all the linear forms, which suggests that the non-linear method estimates the Langmuir parameters better than the linear regression. Consequently, the SNE value for the RMSE error function was lower than that of the other error functions, showing that the deviation of calculated parameters based on this error function was less than that of the other error functions.

3.2.2. The Freundlich isotherm

The Freundlich expression is an empirical equation based on sorption on a heterogeneous surface, suggesting that binding sites are not equivalent. Table 6 shows the Freundlich isotherm parameters based on different error functions. The predicted values based on R^2, χ^2, and ERRSQ were very close to each other, whereas for S_{RE} and MPSD these values were different. The minimum SNE value was obtained for the χ^2 set, which shows the optimum values for $K_{\mathrm{F}} = 16.0418$ and $1/n = 0.74375$. The individual constants, K_{F} and $1/n$, are significantly different from those obtained by the linear error analysis approach; moreover, the R^2 value of the non-linear approach was greater than that of the linear method, which emphasizes the change in the error structure after linearization. Finally, the data obtained by non-linear regression based on the χ^2 error function illustrated that the Freundlich model fitted the experimental data well.

3.2.3. The Temkin isotherm

The Temkin isotherm corresponds to adsorption on strongly heterogeneous equilibrium surfaces. Table 7 shows the non-linearly fitted equilibrium data and error deviations of Hg(II) sorption onto $ZnCl_2$-MCM-41, based on the Temkin isotherm. Values of the R^2, RMSE, and ERRSQ sets are similar, while the values associated with the χ^2, S_{RE}, and MPSD sets are different. The χ^2 set values have the lowest SNE value of the error sets. The model parameters K_{T} and b, which were predicted by the R^2, RMSE, and ERRSQ sets, were very close to the values obtained by the linear

Table 5
The Langmuir isotherm parameters and error deviation data related to the adsorption of Hg(II) onto $ZnCl_2$–MCM-41 obtained by non-linear regression method

	Reference error function					
Error function	R^2	χ^2	RMSE	S_{RE}	MPSD	ERRSQ
q_{m}	202.061	202.503	202.061	202.562	201.197	202.061
K_{L}	0.08491	0.08456	0.08491	0.08417	0.08543	0.08491
R^2	0.99998	0.99998	0.99998	0.99997	0.99998	0.99998
χ^2	0.00540	0.00525	0.00540	0.00676	0.00600	0.00540
RMSE	0.20481	0.20869	0.20481	0.26966	0.22559	0.20481
S_{RE}	0.85528	0.83615	0.85516	0.73479	0.87286	0.85523
MPSD	1.17516	1.20925	1.17521	1.38301	1.16347	1.17519
ERRSQ	0.12584	0.13065	0.12584	0.21815	0.15267	0.12584
SNE	4.96475	4.98173	4.96464	5.841809	5.265245	4.96471

Table 6
The Freundlich isotherm parameters and error deviation data related to the adsorption of Hg(II) onto $ZnCl_2$–MCM-41 obtained by non-linear regression method

Error function	Reference error function					
	R^2	χ^2	RMSE	S_{RE}	MPSD	ERRSQ
K_F	18.0324	16.0418	18.0030	13.7873	14.7700	18.0030
$1/n$	0.68950	0.74375	0.69001	0.78865	0.80268	0.69000
R^2	0.99523	0.99204	0.99523	0.98368	0.97307	0.99523
χ^2	2.45510	1.43619	2.42910	2.82639	2.49399	2.42895
RMSE	3.34060	4.32126	3.34031	6.23446	8.02589	3.34031
S_{RE}	20.6064	12.8618	20.4314	9.09249	13.3475	20.4306
MPSD	34.0190	18.7271	33.7938	16.3448	13.0505	33.7926
ERRSQ	33.4783	56.0199	33.4731	116.606	193.245	33.4731
SNE	4.45811	3.50789	4.433731	4.29031	4.89149	4.43360

Table 7
The Temkin isotherm parameters and error deviation data related to the adsorption of Hg(II) onto $ZnCl_2$–MCM-41, obtained by non-linear regression method

Error function	Reference error function					
	R^2	χ^2	RMSE	S_{RE}	MPSD	ERRSQ
K_T	2.45524	3.67081	2.39254	5.08069	4.77289	2.39256
b	89.8117	129.550	89.8114	201.421	190.920	89.8115
R^2	0.91094	0.83756	0.91004	0.69272	0.70635	0.91004
χ^2	48.9745	21.1231	51.3257	35.2175	32.7214	51.3250
RMSE	15.1937	21.3793	15.1666	34.0356	32.7664	15.1666
S_{RE}	89.9404	42.4279	90.1825	28.0783	28.6556	90.1822
MPSD	157.486	57.7230	164.360	39.2780	38.7682	164.358
ERRSQ	692.541	1,371.23	690.078	3,475.27	3,220.91	690.078
SNE	4.55508	3.17628	4.64418	3.99768	3.85684	4.64415

regression method. However, the values for the optimum parameter set χ^2 were significantly different from the linearized values. The linear form of the R^2 value was greater than the optimum non-linear form (χ^2 set), but it should be noted that a high coefficient of determination does not necessarily indicate a better fit. For instance, the R^2 value of the ERRSQ set is higher than that of the χ^2 set, but sum of the normalized error of the χ^2 set was lower than that of the ERRSQ set, indicating that the χ^2 set presented the optimum parameters for the Temkin isotherm. Finally, the significant differences among the values obtained from different error function sets and the great difference between the values of the optimum set of the non-linear method (the χ^2 set) and the linear form of the Temkin isotherm show the inability of this equilibrium model to predict the behavior of Hg(II) sorption onto $ZnCl_2$-MCM-41.

3.2.4. The Sips isotherm

Sips proposed an equation that combines the Freundlich and Langmuir isotherms [16]. Sips constant parameters and error deviations by non-linear regression are listed in Table 8. According to this table:

(1) The SNE of the χ^2 set was lower than that of other sets.
(2) The R^2 values for all sets were sufficiently high.
(3) The χ^2 set parameters were close to the linear method values.
(4) The S_{RE} set parameters have the most deviation from optimum amounts.

The constant parameter (n) was very close to 1, which indicates that the Sips isotherm follows the Langmuir

Table 8
The Sips isotherm parameters and error deviation data related to the adsorption of Hg(II) onto $ZnCl_2$–MCM-41, obtained by non-linear regression method

	Reference error function					
Error function	R^2	χ^2	RMSE	S_{RE}	MPSD	ERRSQ
q_m	197.768	202.867	197.738	213.231	209.382	197.768
K_S	0.08626	0.08442	0.08627	0.07974	0.08162	0.08626
$1/n$	1.01182	0.99922	1.01190	0.98001	0.98824	1.01182
R^2	0.99999	0.99999	0.99999	0.99988	0.99994	0.99999
χ^2	0.00843	0.00523	0.00847	0.01750	0.00801	0.00843
RMSE	0.17036	0.21411	0.17036	0.53162	0.36031	0.17036
S_{RE}	1.08793	0.82889	1.09116	0.52951	0.76549	1.08761
MPSD	2.57953	1.42943	2.58867	1.37007	1.07528	2.57946
ERRSQ	0.08707	0.13753	0.08707	0.84787	0.38947	0.08707
SNE	3.89837	3.17564	3.90714	5.01441	3.71169	3.89805

assumptions, and the surface of the sorbent ($ZnCl_2$-MCM-41) is homogeneous.

3.2.5. The Redlich–Peterson isotherm

The Redlich–Peterson isotherm parameters and error deviations from the non-linear regression method are presented in Table 9. According to the results, the highest R^2 value was attained for the R^2, χ^2, RMSE, and ERRSQ sets, while the lowest SNE value was obtained for the χ^2 set. The S_{RE} set parameters have the most deviation from the optimum values, and a significant difference exists between linear and non-linear estimated values. It is clear that linearization has a major impact on the R–P isotherm error structure. The results also show that the non-linear regression method is much more reliable than the linear method.

3.2.6. The Toth isotherm

Another three-parameter empirical equation is the Toth isotherm model, which is able to describe both homogenous and heterogeneous adsorption systems [14]. The Toth isotherm constants, namely q_m, K_{T0}, and μ, as well as the values related to the error functions, are tabulated in Table 10. The lowest SNE value was obtained for the χ^2 set of parameters. The maximum adsorption capacities (q_m) of the other sets are significantly different from what was obtained for the χ^2 set.

Table 9
The R–P isotherm parameters and error deviation data related to the adsorption of Hg(II) by $ZnCl_2$–MCM-41 obtained by non-linear regression method

	Reference error function					
Error function	R^2	χ^2	RMSE	S_{RE}	MPSD	ERRSQ
K_{RP}	16.7647	17.0306	16.7661	17.2341	17.3463	16.7655
a_{RP}	0.07040	0.08034	0.07046	0.09759	0.09549	0.07043
β	1.05514	1.01585	1.05491	0.95123	0.96187	1.05499
R^2	0.99999	0.99999	0.99999	0.99988	0.99995	0.99999
χ^2	0.00691	0.00497	0.00689	0.01777	0.00829	0.00691
RMSE	0.13932	0.17521	0.13932	0.52257	0.32980	0.13932
S_{RE}	1.00130	0.81654	0.99972	0.67732	0.89283	1.00034
MPSD	2.40620	1.66120	2.40170	1.75033	1.29125	2.40350
ERRSQ	0.05823	0.09209	0.05823	0.81926	0.32630	0.05823
SNE	4.72261	4.01363	4.71648	6.19760	4.74922	4.71961

The constant μ shows the state of heterogeneity/homogeneity of the sorption process: $\mu = 1$, which describes a completely homogeneous system and any deviations from the value 1 are attributed to a heterogeneous sorption system. For all error sets, the amount of μ was very close to unity, especially for the χ^2 set, which reconfirms the homogeneity of Hg(II) sorption onto $ZnCl_2$-MCM-41. In fact, similar to the Sips isotherm, if $\mu = 1$ (a homogeneous system), then the Toth isotherm transforms into the Langmuir isotherm model.

3.2.7. The Khan isotherm

The Khan isotherm is a three-parameter model for which the parameters cannot be estimated through linear regression. As a result, a non-linear regression method is required in order to fit this isotherm and subsequently find the parameters. The constant γ shows the heterogeneity of the sorption system. Like other isotherms, this isotherm converts to the Langmuir isotherm model when γ is equal to 1. The Khan isotherm constants and error values, which are determined by non-linear regression based on different error functions, are presented in Table 11. According to the SNE values, the χ^2 set parameters are the optimum values to describe Hg(II) sorption onto $ZnCl_2$-MCM-41. For the optimum set, γ is close to unity, which proves the homogeneity of the Hg(II) sorption system. The highest deviation from the optimum parameters was obtained for the MPSD set. The R^2 values in all sets were very high (more than 0.9999), while isotherm constants were largely different, indicating the unreliability of the coefficient of determination for data fitting.

3.3. The best isotherm

In Section 3.2, various isotherms were fitted to the experimental data of Hg(II) sorption onto $ZnCl_2$–MCM-41 using non-linear regression methods. The optimum set of error values (determined based on the lowest SNE value) is listed in Table 12 for each isotherm, in order to specify the one with the best fit for experimental data. Interestingly, the optimum set of errors for the Langmuir model was RMSE, while for other isotherms was χ^2. The primary criterion to find the best-fitting isotherm was SNE, meaning that the lower the SNE value, the better the model fits experimental data. The Khan isotherm has the optimum value of errors in most cases (highlighted in Table 12), but the lowest SNE value was obtained for the Langmuir isotherm model. Except for the Freundlich and Temkin isotherms, the SNE values of other isotherms were very close to each other. As mentioned in the previous sections, the heterogeneity parameters of the Sips ($n = 1.000781$), R–P ($\beta = 1.01585$), Toth ($\mu = 1.01772$), and Khan ($\gamma = 1.09585$) isotherms were very close to unity, the point at which these isotherms convert to the Langmuir model. Therefore, it is not surprising that the Langmuir model has the best fit of the data, as it can include other isotherms' results. Hence, it is concluded that the adsorption of Hg(II) onto $ZnCl_2$–MCM-41 is a monolayer homogeneous sorption process, and the maximum adsorption

Table 10
The Toth isotherm parameters and error deviation data related to the adsorption of Hg(II) onto $ZnCl_2$–MCM-41 obtained by non-linear regression method

	Reference error function					
Error function	R^2	χ^2	RMSE	S_{RE}	MPSD	ERRSQ
q_m	189.386	198.791	189.401	205.974	216.286	189.549
K_{T0}	13.4358	12.1854	13.4358	11.3554	10.8213	1.07011
μ	1.07126	1.01772	1.07123	0.97705	0.94464	1.05499
R^2	0.99999	0.99999	0.99999	0.99987	0.99995	0.99999
χ^2	0.00699	0.00506	0.00701	0.01555	0.00848	0.00687
RMSE	0.14384	0.18163	0.14384	0.55771	0.34161	0.14392
S_{RE}	1.00682	0.82571	1.00765	0.73640	0.88068	0.99734
MPSD	2.40239	1.63886	2.40440	1.74892	1.26278	2.37309
ERRSQ	0.06207	0.09897	0.06208	0.93311	0.35009	0.06207
SNE	3.77228	3.25818	3.77463	5.45807	3.93219	3.74319

Table 11
The Khan isotherm parameters and error deviation data related to the adsorption of Hg(II) onto $ZnCl_2$–MCM-41 obtained by non-linear regression method

	Reference error function					
Error function	R^2	χ^2	RMSE	S_{RE}	MPSD	ERRSQ
q_m	282.592	231.356	278.846	260.723	173.079	280.502
b_k	0.05962	0.07359	0.06046	0.06512	0.09973	0.06009
γ	1.26227	1.09585	1.25012	1.19797	0.90213	1.25550
R^2	0.99999	0.99999	0.99999	0.99998	0.99996	0.99999
χ^2	0.00599	0.00467	0.00583	0.00578	0.00764	0.00590
RMSE	0.12724	0.15766	0.12724	0.22040	0.29183	0.12740
S_{RE}	0.92822	0.78031	0.91635	0.78014	0.90559	0.92164
MPSD	2.25091	1.69233	2.21208	1.83705	1.36401	2.22936
ERRSQ	0.04857	0.07457	0.04882	0.14572	0.25550	0.04857
SNE	4.41014	4.03586	4.36127	4.74517	5.58157	4.38271

Table 12
The optimum error deviation sets obtained from different isotherms by non-linear regression

	Isotherm						
Error function	Langmuir	Freundlich	Temkin	Sips	R-P	Toth	Khan
R^2	0.99998	0.99204	0.83756	0.99999	0.99999	0.99999	0.99999
χ^2	0.00540	1.43619	21.1231	0.00523	0.00497	0.00506	0.00467
RMSE	0.20481	4.32126	21.3793	0.21411	0.17521	0.18163	0.15766
S_{RE}	0.85516	12.8618	42.4279	0.82889	0.81654	0.82571	0.78031
MPSD	1.17521	18.7271	57.7230	1.42943	1.66120	1.63886	1.69233
ERRSQ	0.12584	56.0199	1371.23	0.13753	0.09209	0.09897	0.07457
SNE	1.05043	1.93059	5.83756	1.05466	1.05652	1.05666	1.05535

capacity (monolayer capacity sorption), q_m, is 202.061 mg g^{-1}.

3.4. Adsorption capacity

Along with sorbent cost and reusability, adsorption capacity is one of the main comparison factors for sorption capability. Under similar conditions, the highest adsorption capacity characterizes the best sorbent for a particular process. The adsorption capacity is calculated based on Eq. (1). Thus, q_e is strongly dependent on the C_0, V, and m variables. Hence, comparisons of sorbents' ability to adsorb Hg(II) based on q_e must be done under similar conditions. The capacities of different sorbents for the sorption of Hg(II), as reported in some of the latest studies, are listed in Table 13.

As can be observed, Hg(II) initial concentration ranges and V/m ratios are not the same for different studies. The highest value of V/m ratio was employed in the current work, demonstrating that 1gram of $ZnCl_2$–MCM-41 sorbent treats a larger volume of Hg (II) solution than 1 gram of all other sorbents. The V/m ratio of sorbents listed in Table 13 varies from 0.0045 to 3.0. According to Eq. (1), a greater V/m ratio leads to a greater q_e. Conversely, a lower V/m ratio translates into higher sorbent mass (m) used for the treatment of a specific volume of Hg(II) solution. This greater mass leads to more accessible sorption sites and a larger surface area, which finally leads to a greater driving force and higher adsorption. In addition, the initial metal concentration range has a significant role in the determination of q_e. Increasing the initial concentration enhances the mass transfer driving force (concentration gradient), and thus increases q_e. Compared to the literature, the lowest initial Hg(II) concentration was used in our study. Another important point is the number of accessible active sites on the surface of the adsorbent. Hence, the comparison of sorbents based on maximum adsorption

Table 13
Hg(II) adsorption capacities of various sorbents

Adsorbent	C_0 range (mg L^{-1})	$\frac{V}{m}$ (L g^{-1})	q_e (mg g^{-1})	q_m (mg g^{-1})	Refs.
Hybrid mesoporous aluminosilicate	2–14	0.010/0.01/ = 1.0	14	21	[22]
Dithiocarbamate-MCM-41	100–300	0.010/0.05 = 0.2	–	40	[23]
3-Aminopropyl-MCM-41	~4–400	0.5	120	125	[24]
Amino-MCM-41	100–800	0.005/0.01 = 0.50	400	140	[2]
2-Mercaptothiazoline-MCM-41	1.7–2,870	0.030/0.2 = 0.15	120	141	[25]
Thiol-functionalized-MCM-41	100–400	0.05/0.11 = 0.0045	155	164	[26]
1-Allyl-3-propylthiourea-MCM-41	36–3,600	0.010/0.05 = 0.2	–	300	[27]
Mercaptopropyl-MCM-41	10–4,011	0.020/0.02 = 1.0	4,011	750	[28]
$ZnCl_2$-MCM-41	2–50	0.030/0.01 = 3.0	150	202	(This work)

capacity can be considered if all of the accessible active sites of the sorbent are occupied by Hg(II) species. Finally, the results show that $ZnCl_2$–MCM-41 has a notably high monolayer adsorption capacity for Hg (II) removal from aqueous solutions compared to other works in the literature.

3.5. SEM analysis

SEM micrographs for MCM-41 and $ZnCl_2$–MCM-41 are shown in Fig. 2. Scanning electron microscopy (SEM) (KYKY-EM3200 Digital Scanning Electron Microscope) was used to determine the particle morphology and the particle size distribution of the synthesized material. The particle size of both samples varied between 80 and 200 nm, with average sizes of 150 ± 20 nm (MCM-41) and 160 ± 20 nm ($ZnCl_2$-MCM-41). It was clearly visible that most particles were almost perfectly spherical, although some agglomerates were observed. No clear $ZnCl_2$ aggregates were observed, indicating that $ZnCl_2$ was penetrated into the pores of MCM-41. Thus, the effective dispersion of $ZnCl_2$ onto the spherical MCM-41 material with very high surface area was achieved.

3.6. Effect of sorbent dosage

The effect of sorbent dosage on the amount of mercury adsorbed at equilibrium is shown in Fig. 3. The sorption of mercury by $ZnCl_2$–MCM-41 was studied by changing the quantity of sorbent in the test solution, while maintaining other operating conditions constant. The amount of Hg(II) adsorbed at equilibrium decreased from 8.76 to 1.19 mg g^{-1} when sorbent dosage was increased from 0.005 to 0.05 g in 30 mL of the solution. The increase in sorbent dosage at constant concentration of Hg(II) and solution volume increases the number of unsaturated sorption sites. At higher doses of $ZnCl_2$–MCM-41, there is a superficial sorption of metal ions onto the surface of the adsorbent, which lowers the metal concentration in the solution. Therefore, the decrease in the amount of sorbed mercury with increasing sorbent dosage is due to the split in the flux, or the concentration gradient

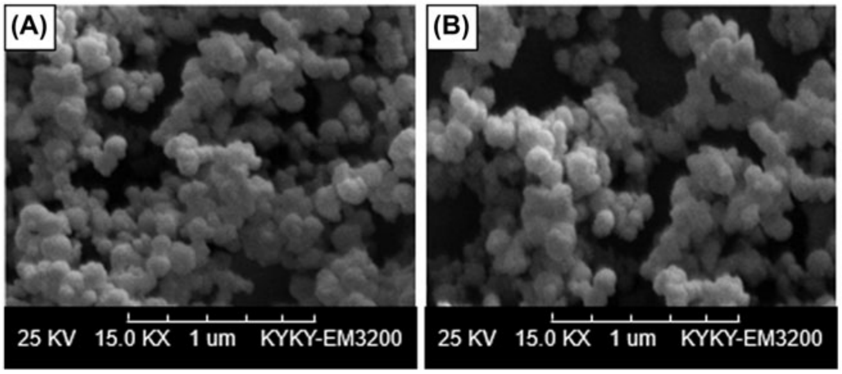

Fig. 2. SEM images of (A) MCM-41 and (B) $ZnCl_2$-MCM-41.

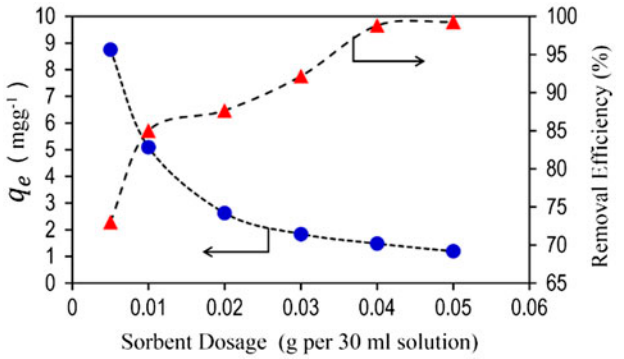

Fig. 3. Effect of adsorbent dosage on the adsorption of Hg (II) onto $ZnCl_2$-MCM-41 (conditions: pH 10, $C_0 = 2$ mg L^{-1}, $T = 20$°C, stirring speed = 300 rpm).

between mercury concentrations in the solution and on the sorbent surface. Additionally, this decrease may be attributed to overlapping or aggregation of sorption sites, resulting in the decrease in total available sorbent surface area for metal ions and an increase in diffusion path length [9,29]. Alternatively, an increase in the $ZnCl_2$–MCM-41 dosage increased the percentage of metal removal from aqueous solution from 73 to 99%. This is mainly attributed to the increase in sorbent surface area and the availability of more sorption sites resulting from the increased dosage of the sorbent [29].

3.7. Influence of ionic strength

Generally, natural waters and wastewaters have different ion concentrations, depending on the water source. The presence of ions at different concentrations may affect the adsorption efficiency of the adsorbents. In this study, the effect of ionic strength on Hg (II) ion adsorption was investigated by adding $NaNO_3$ ions (Fig. 4). The influence of ionic strength on the sorption of Hg(II) by $ZnCl_2$–MCM-41 was studied with a constant initial concentration of 5 mg L^{-1}, sorbent mass of 0.01 g, solution volume of 25 mL, pH value of 10, and temperature of 20°C. The ionic strength of the mercury solution was altered by different doses of $NaNO_3$ (0.01–0.1 M). As expected, the amount of Hg(II) adsorbed decreased as the ionic strength increased, due to the involvement of electrostatic attraction between the adsorbent and adsorbate. An increase in ionic strength resulted in a slight decrease in extraction efficiency. The amount sorbed at equilibrium decreased from 12.6 to 9 mg g^{-1} as the salt concentration increased from 0.01 to 0.1 M, and reached an approximately constant value at concentrations above 0.1 M. This behavior could be attributed to the competition between Hg(II) ions and Na^+ cations for the available sorption sites [30].

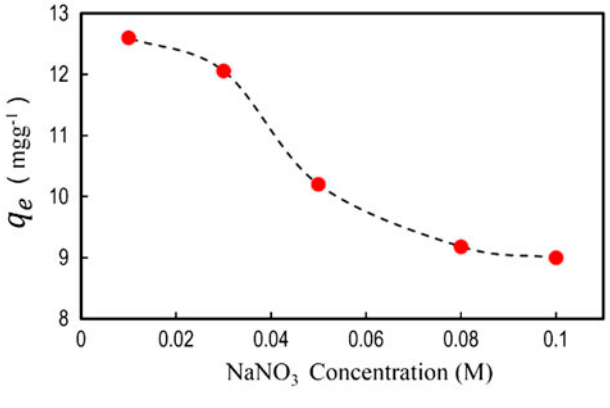

Fig. 4. Effect of ionic strength on the extraction of Hg(II) ions by $ZnCl_2$-MCM-41 (conditions: pH 10, $C_0 = 5$ mg L^{-1}, $T = 20$°C, stirring speed = 300 rpm).

3.8. Adsorption by other metal salts

In order to compare $ZnCl_2$–MCM-41's adsorption selectivity and capacity for Hg(II) ions, other metal salts, including $MgCl_2$, $CuCl_2$, and $CaCl_2$, were used for treating the surface of MCM-41. For this purpose, the method of solvent dispersion in toluene was utilized; this is the same method that was used for adding $ZnCl_2$ on the surface of MCM-41. A ratio of 4 mmol metal salt to 1 g MCM-41 was selected, similar to our previous study [8]. The physicochemical properties of calcined $MgCl_2$–MCM-41, $CaCl_2$–MCM-41, and $CuCl_2$–MCM-41 are listed in Table 14. Fig. 5 shows the adsorption isotherms for $MgCl_2$–MCM-41, $CaCl_2$–MCM-41, $CuCl_2$–MCM-41, and $ZnCl_2$–MCM-41, which were obtained by stirring (300 rpm) 30 ml of Hg(II) solution at initial concentrations of 2, 5, 10, 20, and 50 mg L^{-1} at 20°C and a pH of 6 for 2 h in presence of 0.01 g of sorbent. The Langmuir and Freundlich isotherm parameters of these samples are listed in Table 15. According to the R^2 values, the Langmuir isotherm showed a better fit to the experimental data compared to the Freundlich model for $MgCl_2$–MCM-41, $CuCl_2$–MCM-41, and $ZnCl_2$–MCM-41 sorbents. Hence, the surface of these sorbents was inferred to be homogeneous, and the adsorption of Hg (II) species was determined to be monolayer. However, the R^2 value of the Freundlich isotherm was greater than that of the Langmuir isotherm for $CaCl_2$–MCM-41, which implies that the surface of $CaCl_2$–MCM-41 was heterogeneous and the adsorption of Hg(II) species was not monolayer. The results show that $ZnCl_2$–MCM-41 has a greater Hg(II) adsorption

Table 14
Physicochemical properties of $MgCl_2$–MCM-41, $CuCl_2$–MCM-41, and $CaCl_2$–MCM-41

Samples	S_{BET} ($m^2 g^{-1}$)	V_p ($cm^3 g^{-1}$)	d_{BJH} (nm)	d_{avg} (nm)
$MgCl_2$–MCM-41	650	0.39	2.29	2.33
$CuCl_2$–MCM-41	584	0.43	2.33	2.57
$CaCl_2$–MCM-41	620	0.48	2.51	2.88

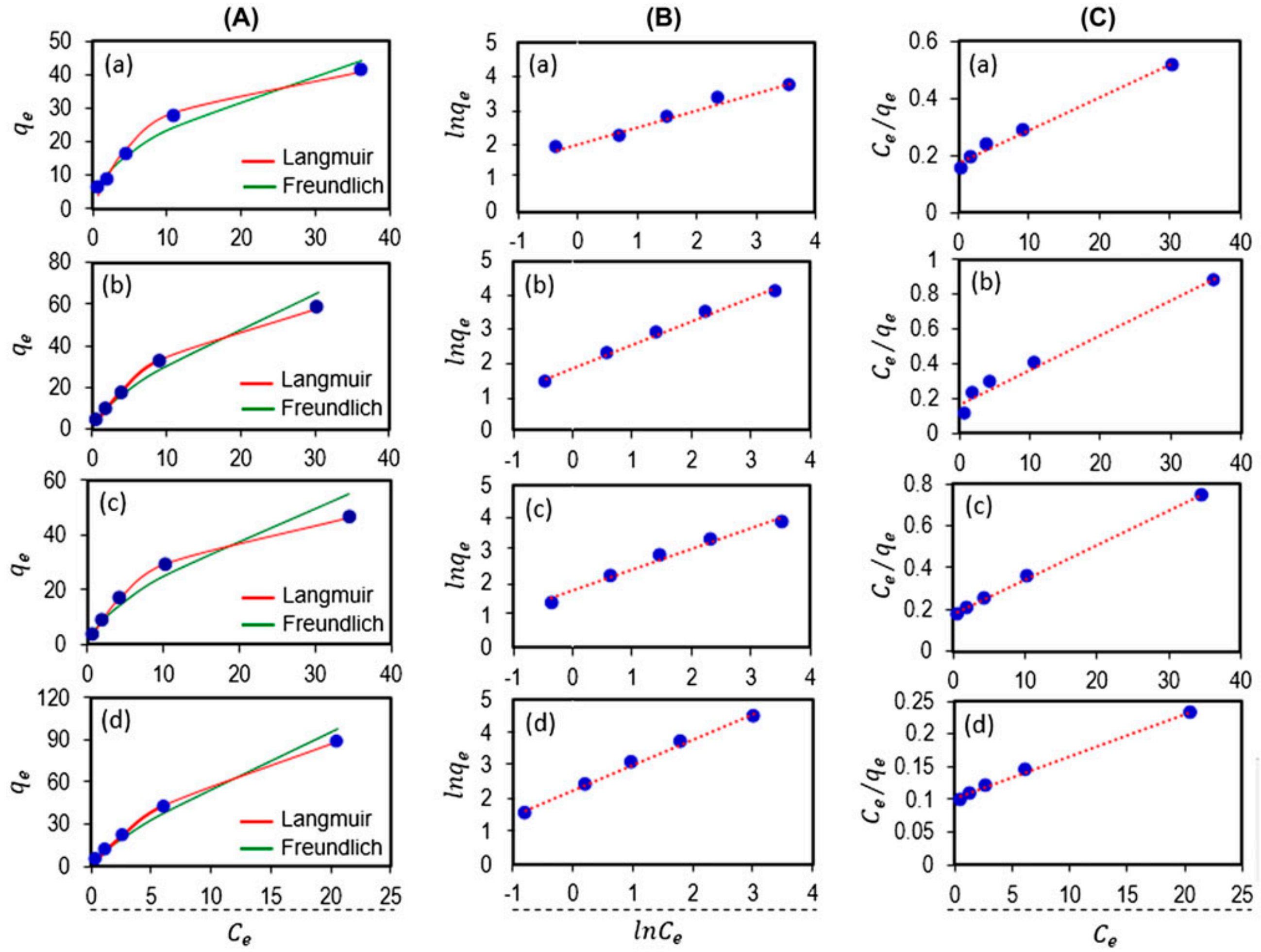

Fig. 5. Adsorption isotherms for: (A) linearized Freundlich, (B) linearized Langmuir, (C) for (a) $MgCl_2$–MCM-41, (b) $CaCl_2$–MCM-41, (c) $CuCl_2$–MCM-41, and (d) $ZnCl_2$–MCM-41.

capacity than $MgCl_2$–MCM-41, $CuCl_2$–MCM-41, and $CaCl_2$–MCM-41.

3.9. Desorption studies

The desorption of Hg(II) species from $ZnCl_2$–MCM-41 using 0.1 M HNO_3 solution was studied in order to provide a better perception of the adsorption mechanisms, and to clarify the feasibility of recovering sorbent and metal ions [31]. The recovery amounts for $ZnCl_2$–MCM-41 at different initial concentrations of Hg(II) ions are listed in Table 16. Based on the results, at all initial Hg(II) concentrations, removal percentages of Hg(II) species were more than 75%. These results indicate that the removal of Hg(II) from water by $ZnCl_2$–MCM-41 mainly took place through affinity

Table 15
The Freundlich and Langmuir isotherms parameters for Hg(II) sorption onto $MgCl_2$–MCM-41, $CuCl_2$–MCM-41, $CaCl_2$–MCM-41, and $ZnCl_2$–MCM-41

	Freundlich isotherm parameters			Langmuir isotherm parameters		
Adsorbent	K_F	$1/n$	R^2	q_m (mg g^{-1})	b (L mg^{-1})	R^2
$MgCl_2$–MCM-41	7.26	0.5013	0.9791	49.89	0.1236	0.9812
$CaCl_2$–MCM-41	6.13	0.6956	0.9907	86.21	0.0684	0.9893
$CuCl_2$–MCM-41	5.70	0.6403	0.9744	60.61	0.0919	0.9991
$ZnCl_2$–MCM-41	9.30	0.7798	0.9831	156.25	0.0630	0.9937

Table 16
Desorption of Hg(II) from $ZnCl_2$–MCM-41 at different Hg (II) initial concentrations

Initial Hg(II) concentration (mg L^{-1})	Hg(II) recovery (%)
2	85
5	83
10	81
20	78
50	76

adsorption. In addition, these results strongly suggest that $ZnCl_2$–MCM-41 is a suitable and reusable sorbent for Hg(II) removal from aqueous solutions.

4. Conclusion

This study successfully exhibited the adsorption of Hg(II) species by the novel and inorganic sorbent $ZnCl_2$–MCM-41. The equilibrium data were analyzed by the Langmuir, Freundlich, Temkin, R–P, Sips, Toth, and Khan isotherms, using linear and non-linear regression methods. In the linear method, the highest value for the coefficient of determination (R^2) specified the best-fitting isotherm, which was obtained by the Langmuir-1 model. On the other hand, for the non-linear method, the best-fitting model was evaluated using seven different error functions. The examination of all these error estimation methods showed that the Langmuir model provides the best fit for the experimental equilibrium data (i.e. the highest R^2 value and the lowest values for χ^2, RMSE, ARE, S_{RE}, MPSD, and ERRSQ). These results indicated that it is not appropriate to use the coefficient of determination of the linear regression method to compare the isotherm models. In addition, it was observed that the non-linear method is a better way to obtain the isotherm parameters. The monolayer adsorption capacity of $ZnCl_2$–MCM-41 based on the Langmuir isotherm was found to be 202.06 mg g^{-1} at 20°C. The SEM images confirmed that MCM-41 and $ZnCl_2$–MCM-41 particles have a spherical shape. Moreover, it was found that increasing the sorbent dosage (while other operating conditions are held constant) leads to an increase in Hg(II) removal efficiency and a decrease in adsorption capacity. In order to compare the Hg(II) adsorption onto MCM-41, three other metal salts, including $MgCl_2$, $CaCl_2$, and $CuCl_2$, were used to modify MCM-41 in a process similar to that used for $ZnCl_2$. Adsorption results show that $ZnCl_2$–MCM-41 has the greatest adsorption capacity among all the studied sorbents. Finally, through the use of 0.1 M HNO_3 solution as desorbent, a minimum 75% recovery of Hg(II) and regeneration of $ZnCl_2$–MCM-41 sorbent was achieved.

Nomenclature

q_e	—	equilibrium sorption amount (mg g^{-1})
C_e	—	equilibrium concentration (mg L^{-1})
q_m	—	maximum adsorption capacity (mg g^{-1})
K_L	—	Langmuir constant (L mg^{-1})
K_F	—	Freundlich constant (an indication of the adsorption capacity) ($mg^{1-(1/n)}$ $L^{1/n}$ g^{-1})
n	—	constant (an indication of favorability of the sorbent)
R	—	universal gas constant (J mol^{-1} K^{-1})
T	—	temperature (K)
B	—	Temkin isotherm constant related to heat of sorption (J mol^{-1})
K_T	—	Temkin isotherm equilibrium binding constant (L g^{-1})
K_S	—	Sips constant related to energy of adsorption ($L^{1/n}$ $mg^{-1/n}$)
K_{RP}	—	Redlich–Peterson isotherm constant (L g^{-1})
a_{RP}	—	Redlich–Peterson isotherm constant (L^{β} $mg^{-\beta}$)
β	—	Redlich–Peterson exponent which lies between 0 and 1
K_{T0}	—	Toth model constant (mg^n L^n)
μ	—	Toth model exponent which lies between 0 and 1
b_K	—	Khan model constants (L mg^{-1})

γ — Khan model exponent which lies between 0 and 1
C_0 — initial metal concentrations (mg L^{-1})
V — volume of the solution (L)
M — dry mass of the employed sorbent (g)
$q_{e,calc}$ — calculated adsorbate concentration at equilibrium (mg g^{-1})
$q_{e,meas}$ — measured adsorbate concentration at equilibrium (mg g^{-1})
$\bar{q}_{e,calc}$ — average of calculated adsorbate concentration at equilibrium (mg g^{-1})
p — number of parameter
n (in Table 2)
— number of data points

References

[1] S.E. Bailey, T.J. Olin, R.M. Bricka, D.D. Adrian, A review of potentially low-cost sorbents for heavy metals, Water Res. 33 (1999) 2469–2479.

[2] M. Puanngam, F. Unob, Preparation and use of chemically modified MCM-41 and silica gel as selective adsorbents for Hg(II) ions, J. Hazard. Mater. 154 (2008) 578–587.

[3] R. Qu, J. Liu, C. Sun, Y. Zhang, C. Ji, P. Yin, Removal and separation of Hg(II) ions from aqueous solutions by macroporous polystyrene-co-divinylbenzene-supported polyamine chelating resins, J. Chem. Eng. Data 55 (2010) 4650–4659.

[4] S.P. Mishra, S.S. Dubey, D. Tiwari, Inorganic particulates in removal of heavy metal toxic ions: IX. Rapid and efficient removal of Hg(II) by hydrous manganese and tin oxides, J. Colloid Interface Sci. 279 (2004) 61-67.

[5] F. Di Natale, A. Erto, A. Lancia, D. Musmarra, Mercury adsorption on granular activated carbon in aqueous solutions containing nitrates and chlorides, J. Hazard. Mater. 192 (2011) 1842–1850.

[6] S.A. Idris, S.R. Harvey, L.T. Gibson, Selective extraction of mercury(II) from water samples using mercapto functionalised-MCM-41 and regeneration of the sorbent using microwave digestion, J. Hazard. Mater. 193 (2011) 171–176.

[7] J. Beck, J. Vartuli, W. Roth, M. Leonowicz, C. Kresge, K. Schmitt, C. Chu, D. Olson, E. Sheppard, A new family of mesoporous molecular sieves prepared with liquid crystal templates, J. Am. Chem. Soc. 114 (1992) 10834–10843.

[8] F. Raji, M. Pakizeh, Study of Hg(II) species removal from aqueous solution using hybrid $ZnCl_2$-MCM-41 adsorbent, Appl. Surf. Sci. 282 (2013) 415–424.

[9] X. Huang, X. Liao, B. Shi, Hg(II) removal from aqueous solution by bayberry tannin-immobilized collagen fiber, J. Hazard. Mater. 170 (2009) 1141–1148.

[10] D.A. Ratkowsky, D.E. Giles, Handbook of Nonlinear Regression Models, M. Dekker New York, NY, 1990.

[11] K.V. Kumar, Optimum sorption isotherm by linear and non-linear methods for malachite green onto lemon peel, Dyes Pigm. 74 (2007) 595–597.

[12] Y.-S. Ho, W.-T. Chiu, C.-C. Wang, Regression analysis for the sorption isotherms of basic dyes on sugarcane dust, Bioresour. Technol. 96 (2005) 1285–1291.

[13] A. Alihosseini, V. Taghikhani, A. Safekordi, D. Bastani, Equilibrium sorption of crude oil by expanded perlite using different adsorption isotherms at 298.15 K, Int. J. Environ. Sci. Technol. 7 (2010) 591–598.

[14] K. Foo, B. Hameed, Insights into the modeling of adsorption isotherm systems, Chem. Eng. J. 156 (2010) 2–10.

[15] F. Raji, M. Pakizeh, Kinetic and thermodynamic studies of Hg(II) adsorption onto MCM-41 modified by $ZnCl_2$, Appl. Surf. Sci. 301 (2014) 568–575.

[16] R. Sips, On the Structure of a catalyst surface, J. Chem. Phys. 16 (1948) 490–495.

[17] J. Zolgharnein, A. Shahmoradi, Characterization of sorption isotherms, kinetic models, and multivariate approach for optimization of Hg(II) adsorption onto Fraxinus tree leaves, J. Chem. Eng. Data 55 (2010) 5040–5049.

[18] Y.-S. Ho, Selection of optimum sorption isotherm, Carbon 42 (2004) 2115–2116.

[19] K.V. Kumar, K. Porkodi, Relation between some two- and three-parameter isotherm models for the sorption of methylene blue onto lemon peel, J. Hazard. Mater. 138 (2006) 633–635.

[20] Y.-S. Ho, Isotherms for the sorption of lead onto peat: Comparison of linear and non-linear methods, Pol. J. Environ. Stud. 15 (2006) 81–86.

[21] K.V. Kumar, Comparative analysis of linear and non-linear method of estimating the sorption isotherm parameters for malachite green onto activated carbon, J. Hazard. Mater. 136 (2006) 197–202.

[22] M. Liu, L.-A. Hou, B. Xi, Y. Zhao, X. Xia, Synthesis, characterization, and mercury adsorption properties of hybrid mesoporous aluminosilicate sieve prepared with fly ash, Appl. Surf. Sci. 273 (2013) 706–716.

[23] K. Venkatesan, T. Srinivasan, P.V. Rao, Removal of complexed mercury by dithiocarbamate grafted on mesoporous silica, J. Radioanal. Nucl. Chem. 256 (2003) 213–218.

[24] Z. Zhu, X. Yang, L.-N. He, W. Li, Adsorption of Hg^{2+} from aqueous solution on functionalized MCM-41, RSC Adv. 2 (2012) 1088–1095.

[25] D. Pérez-Quintanilla, I. Hierro, M. Fajardo, I. Sierra, 2-Mercaptothiazoline modified mesoporous silica for mercury removal from aqueous media, J. Hazard. Mater. 134 (2006) 245–256.

[26] H. Javadian, M. Taghavi, Application of novel polypyrrole/thiol-functionalized zeolite beta/MCM-41 type mesoporous silica nanocomposite for adsorption of Hg^{2+} from aqueous solution and industrial wastewater: Kinetic, isotherm and thermodynamic studies, Appl. Surf. Sci. 289 (2014) 487–494.

[27] V. Antochshuk, M. Jaroniec, 1-Allyl-3-propylthiourea modified mesoporous silica for mercury removal, Chem. Commun. 3 (2002) 258–259.

[28] A. Walcarius, C. Delacôte, Rate of access to the binding sites in organically modified silicates. 3. Effect of structure and density of functional groups in mesoporous solids obtained by the co-condensation route, Chem. Mater. 15 (2003) 4181–4192.

[29] I. Ghodbane, O. Hamdaoui, Removal of mercury(II) from aqueous media using eucalyptus bark: Kinetic and equilibrium studies, J. Hazard. Mater. 160 (2008) 301–309.

[30] T. Anirudhan, L. Divya, M. Ramachandran, Mercury (II) removal from aqueous solutions and wastewaters using a novel cation exchanger derived from coconut coir pith and its recovery, J. Hazard. Mater. 157 (2008) 620–627.

[31] F. Raji, A. Saraeian, M. Pakizeh, F. Attarzadeh, Removal of Pb(II) from aqueous solution by mesoporous silica MCM-41 modified by $ZnCl_2$: Kinetics, thermodynamics, and isotherms, RSC Adv. 5 (2015) 37066–37077.